NOTES AND CORRESPONDENCE

Thermally Forced Surface Winds on an Equatorial Beta Plane*

ZHAOHUA WU, E. S. SARACHIK, AND DAVID S. BATTISTI

Department of Atmospheric Sciences, University of Washington, Seattle, Washington

5 May 1997 and 27 July 1998

ABSTRACT

The vertical structure of the low-level atmospheric response to an elevated large-scale, low-frequency heat source in the Tropics is explored using linear tidal theory on an equatorial beta plane. Through the calculation of the projection of a large-scale, low-frequency thermal source onto the meridional eigenfunctions, the contributions from a set of discrete meridional eigenfunctions with positive equivalent depths, and a continuous spectrum of meridional eigenfunctions with negative equivalent depth, are examined. The positive equivalent depth eigenfunctions have been discussed in some literature while the continuous spectrum of the negative equivalent depth eigenfunctions is new. The authors find that, at lower frequencies, the forced response is mainly supported by those continuous modes for which the absolute values of the negative equivalent depths are neither very small nor very large.

The implications of these results for thermally driven surface winds are discussed and summarized by Eqs. (4.2) and (4.6). In the inviscid case, since the solution associated with the continuous modes with negative equivalent depth is vertically evanescent, it is expected that the vertical energy transfer from the elevated thermal source to the surface is limited. However, in the presence of Newtonian cooling, the continuous modes that contribute significantly to accounting for the large-scale heat source are those modes with moderate values of negative equivalent depth as frequencies goes to zero so that the forced horizontal winds become vertically uniform below the heating. Hence, surface winds can be driven by the elevated heat source in the presence of only linear thermal damping.

1. Introduction

Surface wind anomalies are the main determinant of sea surface temperature anomalies in the Tropics. There have been two mechanisms suggested for generating such surface wind anomalies: 1) forcing by the hydrostatic pressure anomalies in the boundary layer induced by the SST anomalies themselves (Lindzen and Nigam 1987) and 2) thermal forcing from cloud base to the tropopause by anomalies of deep persistent precipitation. Because these mechanisms are highly interrelated (anomalous convergence of low-level moisture leads to anomalies of persistent precipitation and, therefore, to anomalies of thermal forcing) it has not been clear how much of each mechanism contributes to the surface winds. Indeed, for some simple models of surface winds, in particular the Gill (1980) model, the two mechanisms are mathematically indistinguishable (Neelin 1989).

The way to cleanly separate the two mechanisms for generating surface winds is to consider each acting in the absence of the other; indeed, this is what Lindzen and Nigam (1987) have done in examining the first mechanism. To examine the second mechanism, we consider the thermal forcing by a *specified* large-scale precipitation anomaly in the Tropics in a horizontally homogeneous region with no SST anomalies. Any surface wind anomalies forced under these circumstances must have been thermally forced. In order to do the problem correctly, the propagation characteristics of the heat source anomaly from cloud base to the surface have to be considered. Also, since the problem involves propagation and since lids are known to induce artificial standing modes that can induce artificial results throughout a vertical column (Lindzen et al. 1968) the results must be shown to exist independently of an artificial lid imposed at the top.

The thermal heat anomaly will be assumed to have a vertical structure similar to those diagnosed from tropical budget analyses, that is, to begin at cloud base and end near the tropopause with a maximum somewhere in midtroposphere. It will also be assumed to be large scale (order of 1000 km) and change slowly, with assumed periods much longer than a day. It is recognized

* Contribution Number 439 to the Joint Institute for the Study of the Atmosphere and Ocean at the University of Washington.

Corresponding author address: Dr. Zhaohua Wu, JISAO, Box 354235, University of Washington, Seattle, WA 98195-4235.
E-mail: wu@atmos.washington.edu

that propagation problems are significantly influenced by damping so that the effects of various types of damping must be considered.

There is a modest body of literature on this problem considered this way. The simple Gill model cited above is not suitable for looking at this problem because by considering a single vertical mode, the heating is artificially brought right to the surface; the question of the propagation of signals from the bottom of the heat source to the surface, therefore, cannot be considered. Schneider and Lindzen (1977) considered the zonally averaged (Hadley) circulation induced by a zonally averaged thermal heat source and found that the surface winds were basically determined by boundary layer convergence and were hardly modified by the thermal forcing. Indeed, it was on the basis of just such arguments that Lindzen and Nigam decided to look at the boundary layer convergence in the absence of thermal forcing. Geisler (1981) considered a single large-scale steady heat source in a linearized atmospheric GCM and looked at the large-scale wind response. He included cumulus friction and full radiative damping and found that the heat source did indeed generate surface winds. He did not indicate whether or not the surface convergence of moisture generated by the heat source was large enough to sustain the heat source.

The questions, therefore, that need to be answered are the following. 1) Under what circumstances do thermal sources force surface winds in the absence of boundary-forced convergence? 2) Under what circumstances is the anomalous moisture convergence forced by the thermal sources adequate to maintain the thermal source?

We have used a dry spectral primitive equation model and performed a numerical study of these two questions in simplified situations using simplified damping mechanisms and have found that the answer to the first question depends primarily on the form of damping to which the model atmosphere is subjected. In particular, we find that when the damping mechanism is thermally dominated, the winds beneath the thermal source can reach the surface. When the damping is frictionally dominated, the winds are confined to the vertical region of the thermal forcing and cannot reach the surface. Our numerical experiments also show that the three-dimensional structure of the response to the prescribed heating is not sensitive to the heating as long as the maximum heating rate is less than 5 K day^{-1} (corresponding to 20 mm day^{-1} of precipitation) and the heating structure remains the same. However, the amplitude of the response is approximately proportional to the maximum heating rate. These results clearly indicate that the response is essentially linear. While these results will be reported in detail elsewhere, it will be the purpose of this note to give a linear argument for why thermal damping allows surface winds to reach the surface.

The analysis is performed *only* on the equatorial beta plane using variable separation methods very similar to those of the classic paper of Lindzen (1967). As it will be discussed in the next section, the meridional eigenvalue–eigenfunction problem does define a complete set of meridional eigenfunctions. Hence, it is not necessary to use both the equatorial beta plane and the midlatitude beta plane to match the complete solutions on a sphere as was done in Lindzen (1967).

A decomposition including thermal damping leads to Eq. (4.4) below. In the presence of the thermal damping, as the forcing becomes steady (the frequency approaches zero) the vertically uniform response from the forcing to the surface becomes evident from the modes with nonzero equivalent depths. Thus, the proof that thermal forcing can drive surface winds leads to a discussion of the behavior of the equivalent depths as the forcing frequency goes to zero. To our surprise, this discussion is not straightforward and leads to some continuum modes on the equatorial beta plane that, to our knowledge, have not previously been noted in this problem. In the second section, the equivalent depths and corresponding eigenfunctions are discussed. The third examines the projection problem in detail. The fourth section describes how the major result of this note, that thermal damping allows the response to reach the surface, is obtained. The last section summarizes the paper.

2. The equivalent depths and the eigenfunctions

We use the method and notations of Lindzen (1967). There, a meridional decomposition is performed with the nth meridional eigenfunctions satisfying

$$\frac{d^2\Psi_{nk\omega}}{dy^2} + \left(\beta\frac{k}{\omega} - k^2\right)\Psi_{nk\omega} + \frac{(\omega^2 - \beta^2 y^2)}{gh_{nk\omega}}\Psi_{nk\omega} = 0. \tag{2.1}$$

Equation (2.1) is the same as Eq. (25) of Lindzen (1967), where positive k corresponds to westward-propagating waves. Since Eq. (2.1) is discussed in an meridionally infinite domain, the boundary conditions associated with this equation are either the outgoing "radiation condition" or $\Psi_{nk\omega} \to 0$ as $y \to \pm\infty$. For the thermally forced atmosphere we are dealing with, the equivalent depth $h_{nk\omega}$ is the eigenvalue and $(\beta^2 y^2 - \omega^2)$ is the corresponding weighting function. Although the weighting function $(\beta^2 y^2 - \omega^2)$ in Eq. (2.1) is not positive definite in the domain, the singularities at $y = \pm\omega/\beta$ are only apparent since the solutions to Eq. (2.1) for any given ω, k, and $h_{nk\omega}$ are differentiable at these singularities. Hence, Eq. (2.1) and its boundary conditions result in a complete set of eigenfunctions[1] for any given ω, k.

[1] Usually, the completeness of the eigenfunctions of a differential operator is discussed in a finite domain over which the eigenfunctions are all Lebesgue integrable. When the eigenfuncfions are defined in an infinite domain, the principle of analytic continuation should be applied (cf. Friedman 1956). Then, one can apply the theorem of the completeness of the eigenfunctions of an self-adjoint differential operator with only apparent singularities in the interior of an infinite domain in the same way as one can apply it in a finite domain. The completeness theorem that can be applied to Eq. (2.1) and its boundary conditions can be found in Holl (1970).

All the eigenvalues and eigenfunctions can be obtained by finding the Green's function and spectrally representing the differential operator (Friedman 1956). The equivalent depths resulting from Eq. (2.1) and its boundary conditions consist of two types: an infinite number of discrete values of positive equivalent depths (the so-called discrete spectrum) and a continuous spectrum of negative equivalent depth lying on the whole negative real axis (D. Moore 1997, personal communication). The eigenfunctions $\Psi_{nk\omega}$ of different n are mutually orthogonal under the principle of analytic continuation and their orthogonality can be expressed as

$$\int_{-\infty}^{\infty} (\beta^2 y^2 - \omega^2)\Psi_{nk\omega}\Psi_{mk\omega}\, dy = \begin{cases} 0 & m \neq n \\ C_{nk\omega} & m = n, \end{cases} \tag{2.2}$$

where $C_{nk\omega}$ is a function of ω, k, and n.

a. The discrete spectrum

The eigenfunctions corresponding to the discrete spectrum of positive equivalent depth are of the form

$$\Psi_{nk\omega} = \exp\left(-\frac{y^2}{2L^2_{nk\omega}}\right)H_n\left(\frac{y}{L_{nk\omega}}\right), \tag{2.3}$$

where $H_n(y/L_{nk\omega})$ is the Hermite Polynomial of order n (which is a nonnegative integer) and $L_{nk\omega} = [(gh_{nk\omega})^{1/2}/\beta]^{1/2}$ is the characteristic meridional scale corresponding to equivalent depth $h_{nk\omega}$. The relationship between $h_{nk\omega}$ and n is

$$\left(\frac{\omega^2}{gh_{nk\omega}} - k^2 + \beta\frac{k}{\omega}\right)\frac{\sqrt{gh_{nk\omega}}}{\beta} = 2n + 1. \tag{2.4}$$

For the eigenfunctions corresponding to the discrete spectrum, the $C_{nk\omega}$ in Eq. (2.2) can be expressed as

$$C_{nk\omega} = L_{nk\omega}2^{n-1}n!\sqrt{\pi}[(2n+1)\beta^2 L^2_{nk\omega} - 2\omega^2]. \tag{2.5}$$

For the forced waves of low frequency, that is, $\omega \ll \Omega$, one can solve Eq. (2.4) and obtain the equivalent depth $h_{nk\omega}$ in terms of the known parameters for those eigenfunctions corresponding to the discrete spectrum

$$(gh^-_{nk\omega})^{1/2} \approx \frac{\omega^2}{\beta(2n + 1)} \tag{2.6a}$$

and

$$(gh^+_{nk\omega})^{1/2} \approx (2n + 1)\frac{\omega}{k}, \tag{2.6b}$$

which correspond to the "−" and "+" sign solution of Eq. (36) in Lindzen (1967), respectively. It should be noted that the eigenfunctions corresponding to the eigenvalues expressed by (2.6b) exist only for westward-propagating waves.

At low frequencies, the equivalent depths given by Eq. (2.6a) are the counterpart of the equivalent depths of the solutions of the first type to Laplace's tidal equation (Longuet-Higgins 1968); the equivalent depths given by Eq. (2.6b) correspond to the equivalent depths of the solutions of the second type to Laplace's tidal equation [see Figs. 1–6 in Longuet-Higgins (1968)]. As frequencies go to zero, more and more beta-plane modes corresponding to Eq. (2.6b) are equatorially trapped and they become good approximations to the eigenfunctions on a sphere.

b. The continuous spectrum

The equivalent depths resulting from (2.1) and its boundary conditions are continuous when their values are negative. As the frequency goes to zero, Eq. (2.1) can be approximated by

$$\frac{d^2\Psi_{nk\omega}}{dy^2} + \left(\beta\frac{k}{\omega} + \frac{\beta^2 y^2}{g\hat{h}_{nk\omega}}\right)\Psi_{nk\omega} = 0, \tag{2.7}$$

where $\hat{h}_{nk\omega} = -h_{nk\omega}$ is positive. Equation (2.7) can be transformed into the standard Weber equation that defines the Weber parabolic cylinder functions:

$$\frac{d^2\Psi_{nk\omega}}{d\eta^2} + \left(\frac{1}{4}\eta^2 - a\right)\Psi_{nk\omega} = 0, \tag{2.8}$$

where $\eta = y[2\beta/(g\hat{h}_{nk\omega})^{1/2}]^{1/2}$ and $a = -k(g\hat{h}_{nk\omega})^{1/2}/\omega$. Figure 1 plots some solutions (Weber parabolic cylinder functions) for selected values of the parameter a. When $a \leq 0$ (standing or westward-propagating waves), the solutions are oscillatory and asymptotically decaying as η increases. When $a > 0$ (eastward-propagating waves), the solutions increase exponentially before they reach their turning points ($\eta = \pm 2\sqrt{a}$) and become oscillatory and asymptotically decaying afterward. For large positive a, the symmetric and antisymmetric solutions are almost identical everywhere and trivial for small η. When $|\eta| \gg |a|$, all the solutions have their asymptotic envelopes that are proportional to $\sqrt{1/|\eta|}$. More details about the solutions to Eq. (2.8) and their asymptotic properties can be found in Abramowitz and Stegun (1965).

The modes of negative equivalent depths are not artificially induced by approximating a spherical domain with an equatorial beta plane. From Flattery (1967), we know that at low frequencies ($\omega \ll \Omega$) the spherical modes with negative equivalent depth are not trapped in the high latitudes; rather, they have very significant components in the Tropics.

It should be pointed out that the discrete modes with large $h_{nk\omega}$ and the continuous modes with negative equivalent depth are not only mathematically necessary to form a complete set of eigenfunctions on an equatorial beta plane but also physically account for the forcing energy leaked to high latitudes in an inviscid atmosphere.

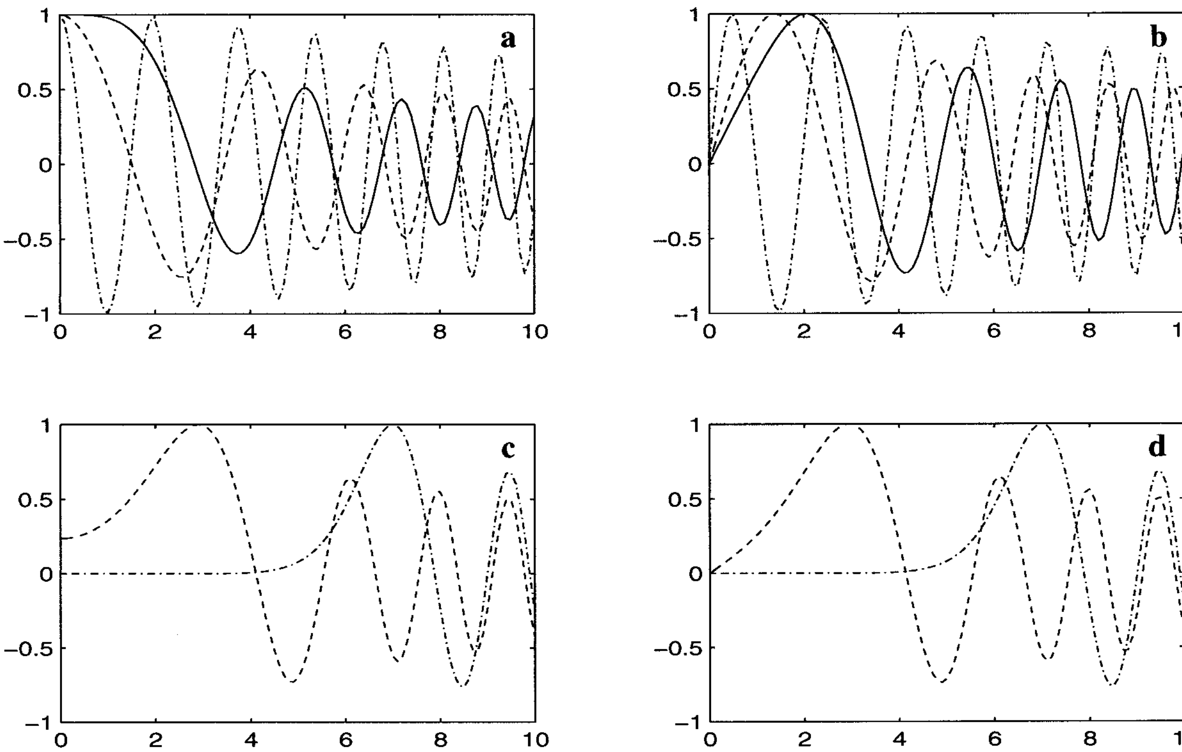

FIG. 1. The normalized Weber parabolic cylinder functions defined by Eq. (2.8) for selected values of the parameter a. (a) and (c) The meridionally symmetric Weber parabolic cylinder functions; (b) and (d) The meridionally asymmetric Weber parabolic cylinder functions. The horizontal axis represents the value of η. (a) and (b) Solid line is for $a = 0$, dashed line is for $a = -1.0$, and dash–dotted line is for $a = -10.0$; (c) and (d) dashed line is for $a = 1.0$, and dash–dotted line is for $a = 10.0$.

3. Projection of forcing onto the modes

We now assume that the external forcing has the form [the left-hand side of the following equation is identical to Eq. (22) in Lindzen (1967)]

$$\tilde{Q} = \frac{-\left(\frac{k}{\omega}\beta y - \frac{\partial}{\partial y}\right)\left(\frac{\partial}{\partial z} - \frac{1}{2H}\right)(\rho_0^{1/2}J)}{\beta^2 y^2 - \omega^2} \approx q_m(z)\chi_m(y), \tag{3.1}$$

where $q_m(z)$ is the vertical structure of the heating and $\chi_m(y)$ is defined as

$$\chi_m(y) = \exp\left(-\frac{y^2}{2L_f^2}\right)H_m\left(\frac{y}{L_f}\right), \tag{3.2}$$

where $\chi_m(y)$ is the parabolic cylander function of order m. The set $\{\chi_m(y)\}$ is complete and is used to expand any meridionally localized function, and L_f is the characteristic meridional scale of the external forcing. If $\tilde{Q}$ meridionally has the shape of a Gaussian distribution [i.e., $m = 0$ in equation (3.2)], $\sqrt{2}L_f$ is the e-folding scale. For the forced problem we are dealing with, the shape of external forcing is prescribed so that L_f is assumed a known constant.

We rewrite

$$\tilde{Q} = \sum_n S_{nk\omega}(z)\Psi_{nk\omega}(y), \tag{3.4}$$

where the summation represents a sum over the discrete spectrum and integration over the continuum.

For the eigenfunctions corresponding to the discrete spectrum, one obtains

$$S_{nk\omega}(z) = \frac{(\beta^2 b - \omega^2)q_m(z)}{C_{nk\omega}}\int_{-\infty}^{\infty}\Psi_{nk\omega}(y)\chi_m(y)\,dy, \tag{3.5}$$

where

$$b = \frac{\frac{2m+1}{L_f^2} - \frac{2n+1}{L_{nk\omega}^2}}{\frac{1}{L_f^4} - \frac{1}{L_{nk\omega}^4}}. \tag{3.6}$$

The detailed derivation can be found in Wu et al. (1997). For the projection coefficients associated with the continuous spectrum, since the corresponding eigenfunctions do not have simple forms, they cannot be given analytically. We will discuss them qualitatively later.

a. The minus sign discrete modes

For a given external forcing, b in Eq. (3.6) is a function of wave frequency ω, zonal wavenumber k, and order n. For large-scale, low-frequency forced waves, one obtains $L^-_{nk\omega}$ as

$$(L^-_{nk\omega})^2 = \frac{\sqrt{gh^-_{nk\omega}}}{\beta} = \frac{\omega^2}{(2n+1)\beta^2}. \qquad (3.7)$$

Equation (3.7) shows that $L^-_{nk\omega} \to 0$ as $\omega \to 0$. So, we have $L^-_{nk\omega} \ll L_f$. When m is not extremely large compared to n,

$$b \approx (2n+1)(L^-_{nk\omega})^2 = \frac{\omega^2}{\beta^2}. \qquad (3.8)$$

Substitution of Eq. (3.8) into Eq. (3.5) gives

$$S^-_{nk\omega}(z) \to 0. \qquad (3.9)$$

Equation (3.9) states that, for a prescribed low-frequency external forcing, the projection onto the minus sign discrete modes approaches zero.

To find the hidden physics in Eq. (3.9), we examine the turning point $y^-_{dnk\omega}$ for the mode $\Psi^-_{nk\omega}$:

$$(y^-_{dnk\omega})^2 = (2n+1)\frac{\sqrt{gh^-_{nk\omega}}}{\beta}. \qquad (3.10)$$

Here $\Psi^-_{nk\omega}$ decays for $|y| > y^-_{dnk\omega}$, so $|y^-_{dnk\omega}|$ can be regarded as the poleward extent of the mode $\Psi^-_{nk\omega}$. For these minus sign discrete solutions, $(y^-_{dnk\omega})^2 = \omega^2/\beta^2$. Hence, $y^-_{dnk\omega}$ is very small and is independent of n; and these modes by themselves cannot account for any response to the external forcing outside the turning points. As $\omega \to 0$, the turning points approach the equator and these minus sign solutions are clearly more and more incomplete.

b. The plus sign discrete modes

As the frequency goes to zero, more and more eigenfunctions corresponding to Eq. (2.6b) on an equatorial beta plane have their counterparts on the spherical earth. Hence, the projections of the external forcing onto these modes must be considered. The turning points for these modes can be expressed as $y^+_{dnk\omega} = (2n+1)\sqrt{\omega/(\beta k)}$. So, at the low-frequency end, when n is not very large, $y^+_{dnk\omega}$ is not very large, and the corresponding eigenfunction $\Psi^+_{nk\omega}$ is still equatorially trapped. However, these modes cannot contribute significantly to the response to a specified external forcing. When n is large and y is limited, $\Psi^+_{nk\omega}$ can be approximated by

$$\Psi^+_{nk\omega} \approx D_n \cos\left(\sqrt{2n+1}\,\frac{y}{L^+_{nk\omega}} - \frac{n\pi}{2}\right)$$

$$= D_n \cos\left(\sqrt{\frac{\beta k}{\omega}}y - \frac{n\pi}{2}\right), \qquad (3.11)$$

where $D_n = 2^{(n+1)/2}(n/e)^{n/2}$, and $L^+_{nk\omega} = [(2n+1)\omega/(\beta k)]^{1/2}$. By considering Eqs. (2.5) and (3.5), one can expect that the projections of external forcing onto these modes go to zero very fast as n increases when n is large, since the $\Psi^+_{nk\omega}$ for different n have the same sinusoidal shape in the Tropics. Hence, only $\Psi^+_{nk\omega}$ of relatively small n contribute to the response to the external forcing. Since the distance of consecutive zeros of $\Psi^+_{nk\omega}$ is independent of n for large n, we can also infer that the plus sign modes with discrete positive eigenvalues do not resolve scales smaller than $\pi\sqrt{\omega/\beta k}$. Hence, the discrete modes can never constitute a complete set.

The dependence of the projections $P_{nk\omega}$ of the external forcing onto the modes of discrete positive equivalent depths as a function of the characteristic scale of the external forcing L_f is shown in Fig. 2, where $P_{nk\omega} = S_{nk\omega}/q_m(z)$. The heat source $\tilde{Q}$ has a Gaussian shape with Gaussian scale L_f and is of unit amplitude. It is clear that for a large range of the characteristic meridional scale of the external forcing L_f, only the $n = 0$ modes are significant. When L_f is large enough, however, the contributions from the plus sign discrete modes with larger characteristic meridional scale $L_{nk\omega}$ (larger n) become nontrivial. This is especially clear in Fig. 2d, where the ratio $P^+_{2k\omega}/P^+_{0k\omega}$ increases as the characteristic scale of the external forcing L_f becomes larger. When L_f is very small, we see that the projections of the external forcing onto the minus sign discrete modes increase as L_f decreases. (The discontinuity at $L_f = 450$ km in panel *c* is due to the change of sign of $P^-_{0k\omega}$ at that point.)

c. The continuous spectrum of modes with negative equivalent depth

The incompleteness of the discrete modes is demonstrated in Fig. 3 where a Gaussian profile is separated into two parts: 1) the part accounted for by an infinite set of the discrete modes and 2) the part accounted for by the continuous modes (which is the difference between the Gaussian profile and the part accounted for by the discrete modes). It is obvious that the continuous eigenfunctions of negative equivalent depth must be included to form a complete set that can be used to decompose the heating and the variables. But so far it is almost impossible to analytically calculate the projections of a heat source onto these eigenfunctions of negative equivalent depth since the solutions to Eq. (2.8) can be expressed only as infinite power series or complex integrals and these solutions are not Lebesgue square integrable in the infinite domain. Thus, instead of a quantitative calculation, a qualitative discussion of the projections onto those modes is presented by considering the properties of the asymptotic solutions.

At a given frequency, $\Psi_{nk\omega}$ is an oscillatory function of y for westward-propagating waves (positive k). When the absolute value of the equivalent depth is very small, a is very small, and the absolute value of η is very large for any nonzero y. Since the solution of $\Psi_{nk\omega}$ in such a case asymptotically decays as $\sqrt{1/|\eta|}$, we can infer that $\Psi_{nk\omega}$ is equatorially trapped when $\hat{h}_{nk\omega}$ is small. Such a

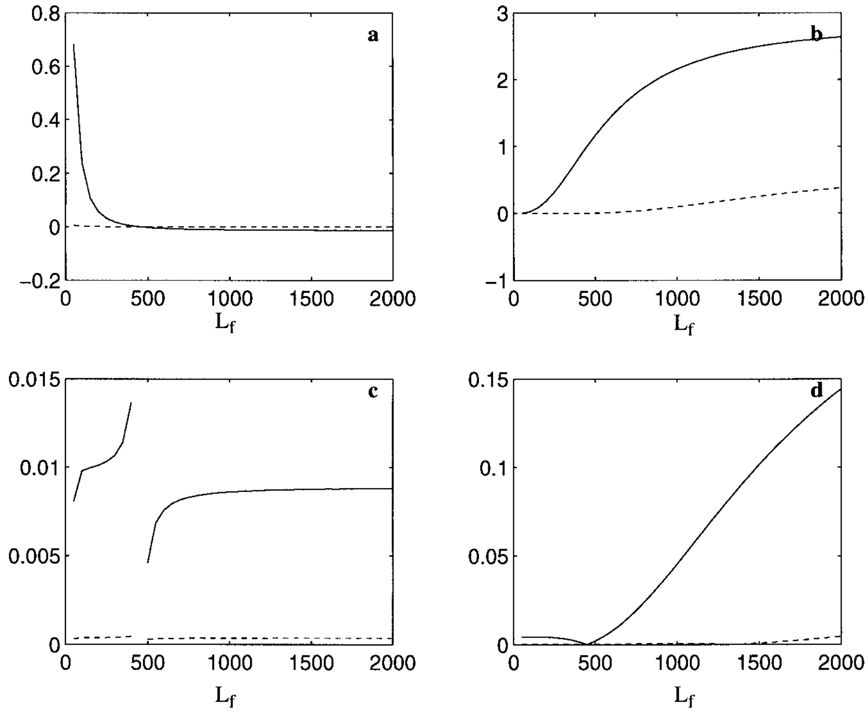

FIG. 2. The projection coefficients as functions of the characteristic meridional scale of external forcing L_f for the modes of zonal wavenumber one and 100-day period. (a) The projection coefficients $P^-_{0k\omega}$ (solid line) and $P^-_{2k\omega}$ (dashed line); (b) the projection coefficients $P^+_{0k\omega}$ (solid line) and $P^+_{2k\omega}$ (dashed line); (c) the ratios $|P^-_{2k\omega}/P^-_{0k\omega}|$ (solid line) and $|P^-_{4k\omega}/P^-_{0k\omega}|$ (dashed line); and (d) the ratios $|P^+_{2k\omega}/P^+_{0k\omega}|$ (solid line) and $|P^+_{4k\omega}/P^+_{0k\omega}|$ (dashed line). In each panel, the horizontal axis represents the characteristic meridional scale of external forcing L_f in kilometers.

eigenfunction can hardly account for the external forcing with a large characteristic meridional scale L_f. When the absolute value of the equivalent depth is very large, from Eq. (2.7) we can infer that $\Psi_{nk\omega}$ is asymptotically proportional to $\exp(i\sqrt{k\beta/\omega}y)$ for any y that is not very large when $\hat{h}_{nk\omega}$ is very large and, therefore, $\Psi_{nk\omega}$ is too wavy at very low frequencies to account for the external forcing. Hence, the eigenfunctions with negative equivalent depths that carry the significant information from the forcing must have a moderate value of $\hat{h}_{nk\omega}$. A similar argument holds for the eastward-propagating waves.

4. Vertical structure equation

The vertical structure equation in Lindzen (1967) is

$$\frac{d^2V_{nk\omega}}{dz^2} + \left(\frac{\kappa}{Hh_{nk\omega}} - \frac{1}{4H^2}\right)V_{nk\omega} = -\frac{\kappa}{H}S_{nk\omega}, \quad (4.1)$$

where $\kappa = R/c_p$ and H is the scale height of the isothermal atmosphere.

For the discrete spectrum, the eigenfunctions that are the valid approximations to the spherical modes generally satisfy $0 < h_{nk\omega} < H$. Hence, the signals excited by the external forcing propagate vertically with vertical wavenumber m, which is approximated by

$$m^2 \approx \frac{\kappa}{Hh_{nk\omega}}. \quad (4.2)$$

The modes corresponding to the continuous spectrum have negative equivalent depths and, thus, they decay away from the heating level. The solutions to Eq. (4.1) are vertically evanescent for these modes.

In the presence of dissipation, how the signals propagate depends on the form of the damping. It is often stated that the distance a forced signal can propagate is characterized by the product of the group velocity of the free wave and damping timescale. At low frequencies, the vertical group velocity for the modes defined by Eqs. (2.6a) and (2.6b) are

$$\left(\frac{d\omega}{dm}\right)^- = C^-_{gz} = \sqrt{\frac{H}{\kappa g}}\frac{\omega^3}{2(2n+1)\beta}, \quad (4.3a)$$

and

$$\left(\frac{d\omega}{dm}\right)^+ = C^+_{gz} = \sqrt{\frac{H}{\kappa g}}\frac{(2n+1)\omega^2}{k}, \quad (4.3b)$$

respectively. The vertical group velocities of zonal wavenumber-one waves are calculated for an isothermal atmosphere with a scale height of 8 km and are presented in Fig. 4. It is clear that for the waves of a period of

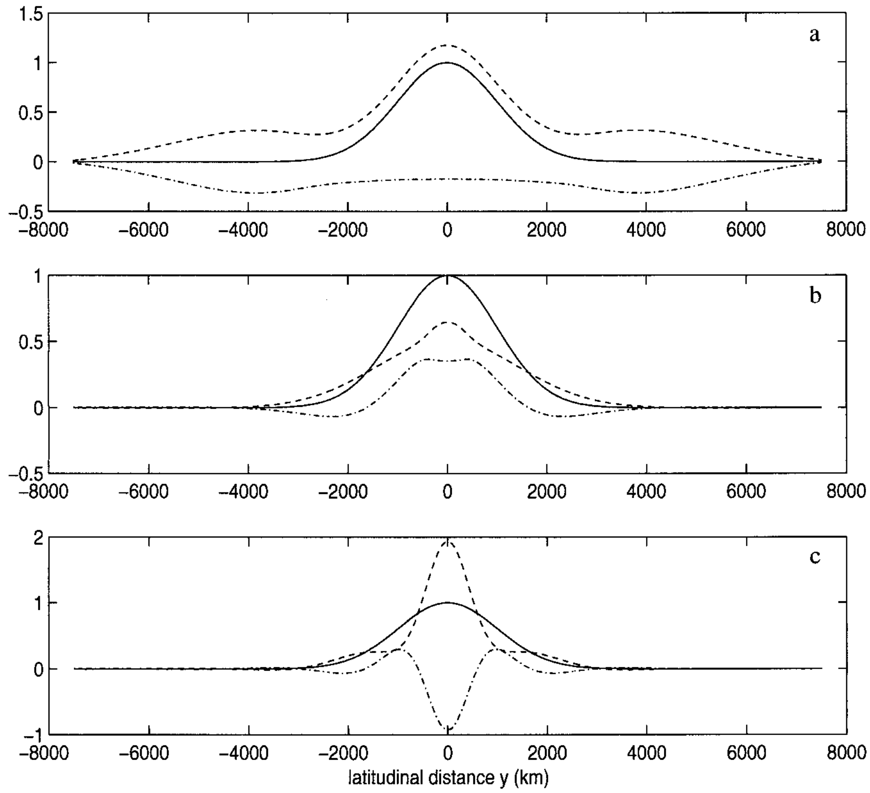

FIG. 3. The projection of a Gaussian profile (with a scale of 1000 km) onto the meridional eigenfunctions. Zonal wavenumber one is used in the meridional structure equation. (a), (b), and (c) correspond to waves of 1-, 10-, and 100-day periods, respectively. In each panel, the solid line is the Gaussian profile, the dashed line is the part of the Gaussian profile that is accounted for by all the discrete modes, and the dash–dotted line is the part that is resolved by the continuous modes.

about 40 days, the plus sign discrete modes can propagate a few hundred meters per day, while the minus sign discrete modes propagate less than 1 m day^{-1}. At high frequencies, the vertical group velocities of all the modes with discrete positive equivalent depth are large. However, since the large-scale heat source does not project onto the low-order plus sign discrete modes significantly at low frequencies, the large group velocities associated with the plus sign discrete modes do not necessarily mean that the response below the forcing level is large. This implies that the continuous modes with negative equivalent depths (which account for most of the vertically standing response) may be the key to explain the significant response below the forcing level.

To what extent the above argument can approximate the dissipative system is difficult to determine. Since the equations are analytically intractable if both thermal damping and momentum damping are added, here we deal with the simplest case in which Newtonian cooling is included as the only damping. Lindzen (1968) first considered a case in which Newtonian cooling is inversely proportional to the density of the atmosphere to study the vertically propagating waves. His results showed that at very high levels (where the Newtonian cooling rate is very large) the amplitude of the horizontal divergence is vertically uniform. When we add a Newtonian cooling term to the thermodynamic equation in Lindzen (1967) and use the same method that he used to separate the equations, the eigenvalue–eigenfunction equation is identical to Eq. (2.1) and the vertical structure equation becomes

$$\frac{d^2V_{nk\omega}}{dz^2} + \left[\frac{\omega\kappa}{(\omega - i\gamma)Hh_{nk\omega}} - \frac{1}{4H^2}\right]V_{nk\omega} = -\frac{\kappa}{H}S_{nk\omega}, \tag{4.4}$$

where $i = \sqrt{-1}$ and γ is the Newtonian cooling rate. When $\omega \rightarrow 0$, we know that the projection of the forcing goes mainly to the modes whose $h_{nk\omega}$ are not zero. Hence, when the thermal damping timescale is around two weeks or shorter, we have $|i\gamma| \gg \omega$, and then we obtain

$$\left|\frac{1}{4H^2}\right| \gg \left|\frac{\omega\kappa}{(\omega - i\gamma)Hh_{nk\omega}}\right| \tag{4.5}$$

for the waves excited by the external forcing. Then, the vertical Eq. (4.4) simplifies to

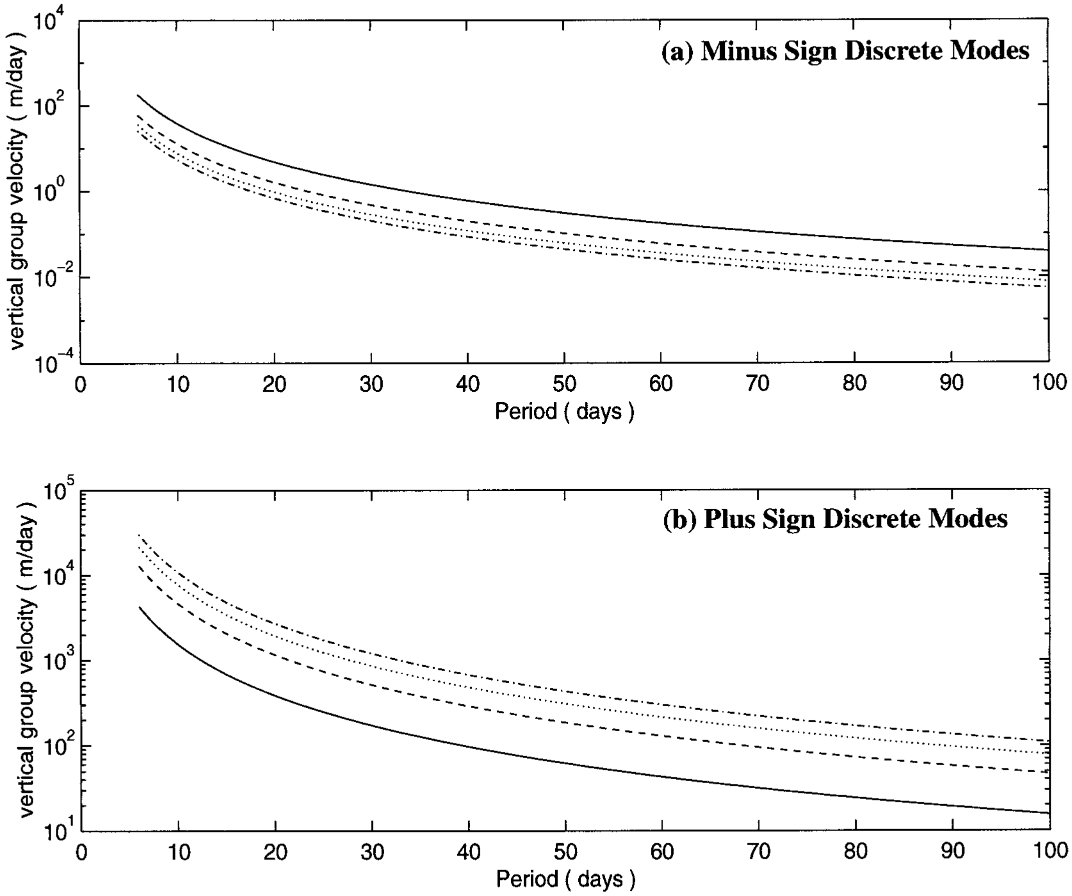

FIG. 4. The vertical group velocity corresponding to (a) minus sign discrete modes and (b) plus sign discrete modes of zonal wavenumber one as a function of wave period. Solid lines correspond to $n = 0$, dashed lines $n = 1$, dotted lines $n = 2$, and dash–dotted lines $n = 3$. The value of the buoyancy frequency N used in this calculation corresponds to an isothermal atmosphere with scale height H of 8 km; the vertical group velocity is plotted in meters per day.

$$\frac{d^2V_{nk\omega}}{dz^2}\frac{V_{nk\omega}}{4H^2} = -\frac{\kappa}{H}S_{nk\omega}. \tag{4.6}$$

Equation (4.6) states that the response to the forcing decays exponentially in the vertical outside of the heating with a decay scale of $\frac{1}{2}H$. Recalling that the variable $V_{nk\omega}$ has already been mass weighted, we conclude that the meridional wind itself must be vertically uniform above and below the heating—in particular, under the convective heating region.

5. Conclusions

In last three sections, we discussed both the latitudinal structure equation and the vertical structure equation in Lindzen (1967). Our emphasis is on the low-level responses to a large-scale low-frequency elevated heat source in the Tropics.

By analyzing the projections of the external forcing onto different modes, we find that all the eigenfunctions corresponding to Eq. (2.6a) shrink to the equator as frequency goes to zero. Hence, these modes are, in general, incapable of resolving an external forcing with a prescribed large meridional scale.

Among the plus sign modes of discrete positive equivalent depths, those modes of large n may not be applied to the spherical domain. It can be shown, however, that the projections of an external forcing onto large n modes are vanishingly small. Hence, the plus sign discrete modes with large n do not contribute to the solution and we need not worry that the equatorial beta-plane modes are not appropriate to the spherical earth. Practically, how many modes of relatively small n should be retained is determined by both the frequency and the characteristic meridional scale of the external forcing.

The complete solution to a meridionally localized heat source in the Tropics includes the modes from a continuous spectrum of negative equivalent depths that have not previously been discussed in the literature. As the frequencies go to zero, the external forcing projects mainly onto these large negative equivalent depth modes. Physically, these modes also account for the linear response at higher latitudes to the imposed tropical heating.

The application of the group velocity argument to a dissipative system is questionable. In general, it is necessary to examine the details of the dissipating processes. It is clear from section 4, however, that adding thermal damping fundamentally changes the vertical structure of the response. Nonetheless, from the vertical structure equation, we can infer that a significant surface wind can be driven by an elevated, large-scale diabatic heating if thermal damping is the dominant dissipating mechanism.

To more completely assess the roles of Rayleigh friction and Newtonian cooling in producing surface wind, we have performed numerical experiments with a dry global spectral atmosphere model. Consistent with the argument in section 4, we find that in the presence of Newtonian cooling, the solutions are characterized by winds that extend vertically away from the heating in a uniform fashion; hence, the Newtonian cooling does allow for a significant surface wind response to a vertically elevated heating. In contrast, when Rayleigh friction dominates, the circulation driven by the elevated heat source is vertically confined to the layer where the heat source is located. The detailed description of this modeling study will be reported in Wu et al. (1998, manuscript submitted to *J. Atmos. Sci.*).

Acknowledgments. This work was supported by a grant from the NOAA/Office of Global Programs to the Stanley P. Hayes Center of the University of Washington. The authors would like to thank Professor K.-K. Tung and the reviewers for helpful and substantive comments.

REFERENCES

Abramowitz, M., and I. A. Stegun, 1965: *Handbook of Mathematical Functions.* Dover, 1064 pp.

Flattery, T. W., 1967: Hough functions. Ph.D. dissertation, Department of Geophysical Sciences, University of Chicago, 168 pp.

Friedman, B., 1956: *Principles and Techniques of Applied Mathematics.* John Wiley and Sons, 315 pp.

Geisler, J. E., 1981: A linear model of the Walker circulation. *J. Atmos. Sci.,* **38,** 1390–1400.

Gill, A. E., 1980: Some simple solutions for heat-induced tropical circulations. *Quart. J. Roy. Meteor. Soc.,* **106,** 447–462.

Holl, P., 1970: The completeness of the orthogonal system of the Hough functions. *Nachr. Akad. Wiss. Göttingen, Math-Phys. Kl., 2,* **7,** 159–168.

Lindzen, R. S., 1967: Planetary waves on beta-planes. *Mon. Wea. Rev.,* **95,** 441–451.

——, 1968: Vertically propagating waves in an atmosphere with Newtonian cooling inversely proportional to density. *Can. J. Phys.,* **46,** 1835–1840.

——, and S. Nigam, 1987: On the role of sea surface temperature gradients in forcing low-level winds and convergence in the Tropics. *J. Atmos. Sci.,* **44,** 2418–2436.

——, E. S. Batten, and J.-W. Kim, 1968: Oscillations in atmosphere with tops. *Mon. Wea. Rev.,* **96,** 133–140.

Longuet-Higgins, M. S., 1968: The eigenfunctions of Laplace's tidal equations over a sphere. *Phil. Trans. Roy. Soc. London,* **262A,** 511–607.

Neelin, J. D., 1989: On the interpretation of the Gill model. *J. Atmos. Sci.,* **46,** 2466–2468.

Schneider, E. K., and R. S. Lindzen, 1977: Axially symmetric steady-state models of the basic state for instability and climate studies. Part I: Linearized circulations. *J. Atmos. Sci.,* **34,** 263–279.

Wu, Z., E. S. Sarachik, and D. S. Battisti, 1997: Forced planetary waves on an equatorial beta-plane. Preprints, *11th Conf. on Atmospheric and Oceanic Fluid Dynamics,* Tacoma, WA, Amer. Meteor. Soc., 6–10.